MCAT Institute Final Report 91-001

ROTORCRAFT APPLICATION OF ADVANCED COMPUTATIONAL AERODYNAMICS

Sharon Stanaway

January 1991

(NASA-CR-187767) ROTORCRAFT APPLICATION OF ADVANCED COMPUTATIONAL AERODYNAMICS Final Report (MCAT Inst.) 8 p CSCL 01A

N91-15987

Unclas
G3/02 0325584

MCAT Institute
San Jose, California

MCAT Institute Final Report 91-001

ROTORCRAFT APPLICATION OF ADVANCED COMPUTATIONAL AERODYNAMICS

Sharon Stanaway

January 1991

MCAT Institute
San Jose, California

Rotorcraft Application of Advanced Computational Aerodynamics

by Sharon Stanaway

Introduction

The objectives of this program is to develop the capability and to compute the unsteady viscous flow around rotor-body combinations. In the interest of tractability, the problem was divided into subproblems: computing the flow around a rotor blade in isolation, computing the flow around a fuselage in isolation, and integrating the pieces. Considerable progress has already been made by others toward computing the rotor in isolation (Srinivasen) and this work has focused on the remaining tasks.

This task required formulating a multi-block strategy for combining rotating blades and nonrotating components (i.e. a fuselage). Then an appropriate configuration was chosen for which suitable rotor body interference test data exists. Next, surface and volume grids were generated and state-of-the-art CFD codes were modified and applied to the problem.

Results

The approach taken here is to analyze the fuselage in isolation (figure 1a), the rotor in isolation (figure 1b), and to combine the two computations using the overset grid software known as Pegasus (figure 1c). This has the advantage that the isolated fuselage grids can be used directly for interactional aerodynamic simulations, thus greatly simplifying the constrains of the grid generation process. The rotor model can first be represented by boundary conditions in the rotor plane, shown in figure 1b by a red semi-circle in the center of the grid, where the grid is held fixed (i.e. an actuator disk model). A more sophisticated model can then be substituted until the ultimate case of a viscous solution of the rotor in the rotating grid is included.

A suitable configuration was chosen for which experimental data exists with and without a rotor. The configuration of figure 2 was chosen because of the current and ongoing full scale rotor-body interaction experiments which were in progress at NASA Ames (fig. 2a) and the available small scale test data from the 7 by 10 foot tunnel at Ames (fig. 2b).

The body alone without the strut supports was modeled with a surface grid and a corresponding volume grid using a hyperbolic grid generator, HYGRID. At zero angle of attack, the Navier Stokes solutions agreed reasonably well with panel method results and

with the 7 by 10 foot data (figure 3), however, it did not compare well with the 40 by 80 foot tunnel data. The reason for this is attributed to the significant strut interference of this test. It was evident from this that the struts need to be included in the computation in order to obtain close agreement with the large scale results.

Navier Stokes calculations proceeded on the isolated body for relatively high angles of attack for the laminar and turbulent cases shown in figure 4a and 4b, respectively. The surface skin friction patterns were compared to oil flow patterns and showed qualitative agreement (figure 4c).

Surface grid generation and panel method solutions were generated as first approximations to the 40 by 80 test configuration. These results are shown in figure 5. This surface definition is then being used to generate suitable viscous grid for Navier Stokes calculations.

The actuator disk model was imposed in the F3D code using the "Fortified Approach" (Van Dalsem) having the advantage that the boundary conditions are applied in the interior of the domain and are therefore implicit. The correct contraction ratio was obtained for the solution shown in figure 6 where the colors represent velocity, the disk is shown from the side by the thick red line and the streamlines are shown going from left to right.

Finally, the rotor and body have been combined in Pegasus and solutions for the interactional aerodynamics problem are next on the agenda.

References

Smith & Betzina 1986 "Aerodynamic loads induced by a rotor on a body of revolution," J. AHS 31, 1.

Srinivasen, G.R., Baeder, J.D., Obayashi, S., McCroskey, W.J., 1990, "Flowfield of a Lifting Hovering Rotor — A Navier-Stokes Solution", Sixteenth European Rotorcraft Forum, Glaskow, Scotland.

Van Dalsem, W.R., and Steger, J.L. 1986 "Fortified Navier Stokes Approach," Workshop on Computational Fluid Dynamics, Institute of Nonlinear Sciences, U. of CA, Davis.

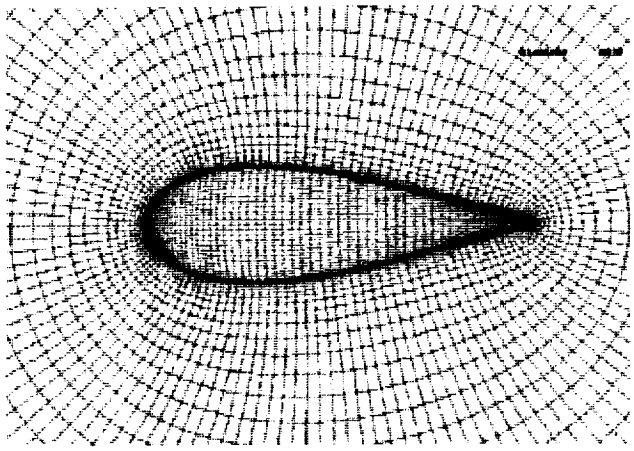

Figure 1a. Isolated body grid.

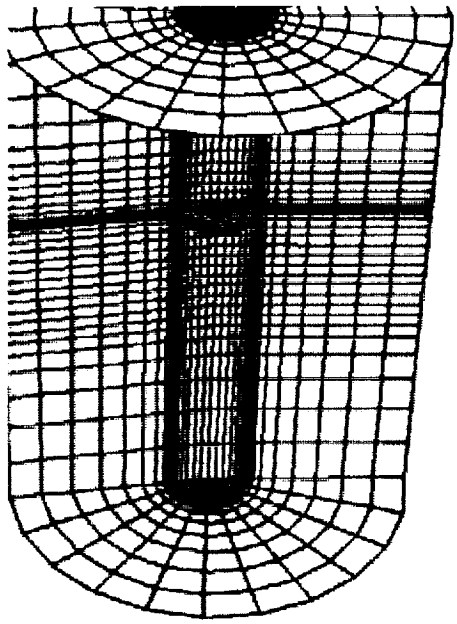

Figure 1b. Isolated rotor grid.

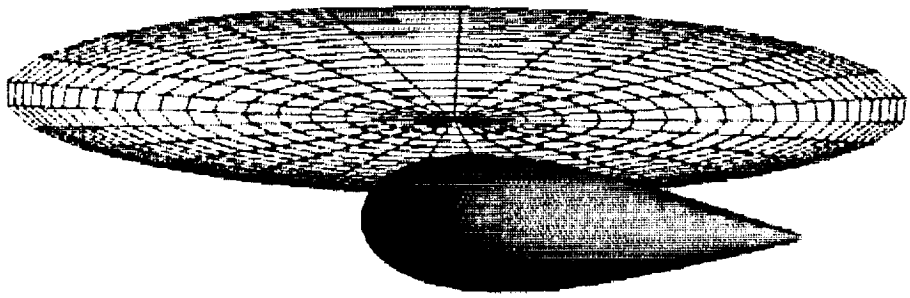

Figure 1c. Combined rotor and body using Chimera/F3D

Figure 2a. 40 by 80 foot rotor-body interference wind tunnel test (Re = 27,000,000).

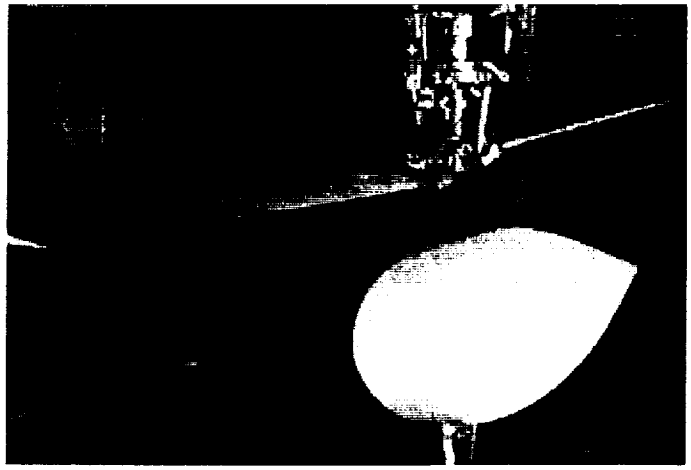

Figure 2b. 7 by 10 foot rotor-body interference wind tunnel test (Re = 4,900,000).

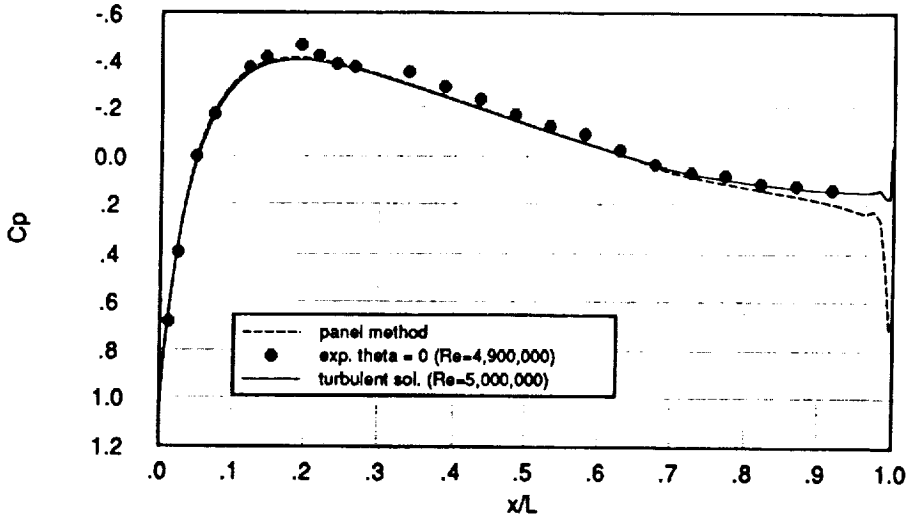

Figure 3. Pressure coefficient along body centerline at zero degrees angle of attack.

Figure 4a. Navier–Stokes calculation, Re = 100,000, laminar flow, alpha = 24 deg., M = 0.2.

Figure 4b. Navier–Stokes calculation, Re = 27,000,000, turbulent flow, alpha = 17 deg., M = 0.18.

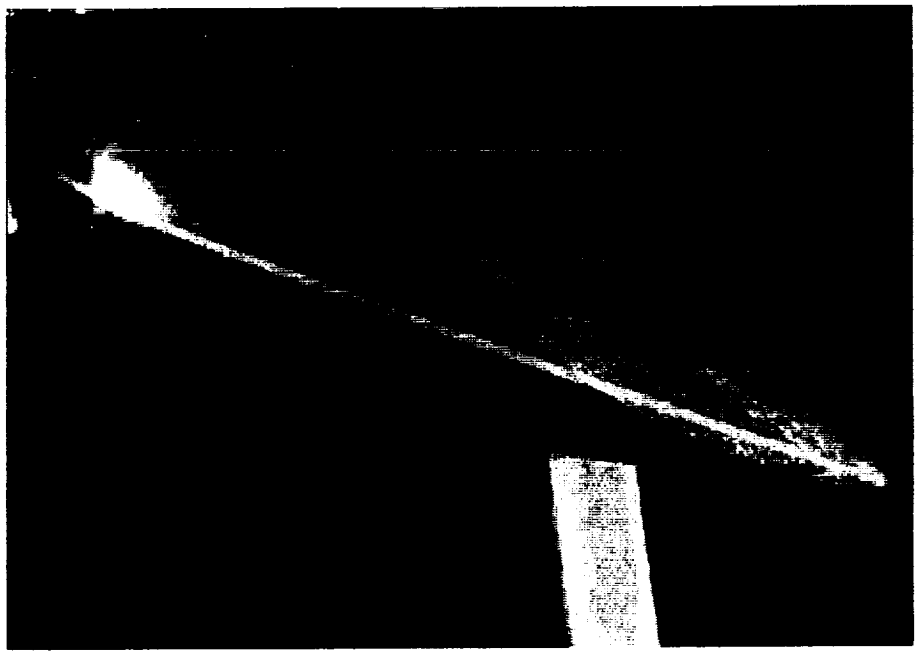

Figure 4c. Oil flow visualization, Re = 500,000, turbulent flow, alpha = 24 deg.

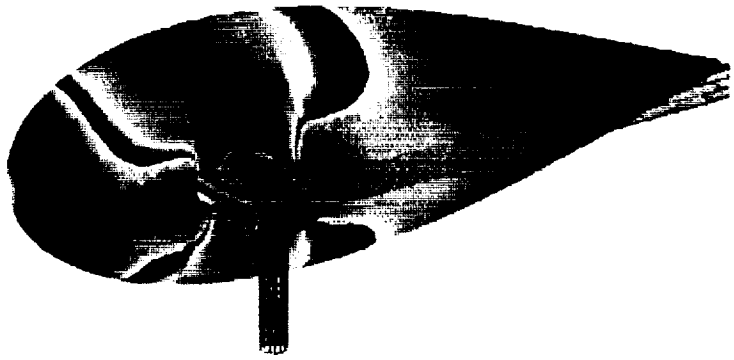

Figure 5. Panel method calculation on the body with wing stubs and strut supports.

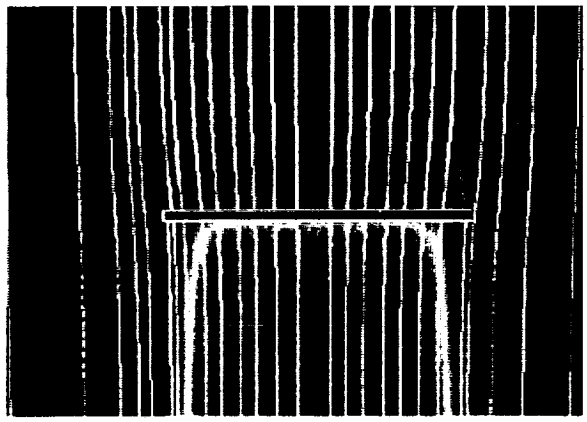

Figure 6. Horizontal slice through an actuator disk rotor simulation of the Navier–Stokes equations.